

# The application of a curing front model to simulate healing in a cementitious microbial system.

Anthony Jefferson<sup>1\*</sup> and Brubeck Freeman<sup>1</sup>

<sup>1</sup>School of Engineering, Cardiff University, The Parade, Cardiff CF24 3AA, UK

**Abstract.** This study investigates the ability of a coupled finite element model to simulate Microbially Induced Calcium Carbonate Precipitation (MICP) and associated healing behaviour in cementitious samples. This recent coupled 3D model was first developed for simulating the behaviour of autonomic healing systems in cementitious structural elements. It employs a cohesive zone constitutive model for simulating the damage-healing behaviour of an embedded interface within 3D continuum elements. Fluid flow is simulated using a mass balance equation and Darcy's law. Healing is computed via a generalised curing front model that simulates the accumulation of healed material within a crack. The research reported in this article demonstrates that the curing front model can be calibrated to predict healing from MICP in cementitious specimens with good accuracy.

## 1 Introduction

A comprehensive progress review of research on the numerical simulation of self-healing cementitious materials in 2018 [1] concluded that many models for self healing cementitious materials (SHCMs) had been validated using either limited sets of experimental data or no test data at all. It also highlighted the fact that relatively little work had been published on fully coupled models for biomimetic cementitious material that bring together reactive chemical transport and mechanical behaviour, with a few notable exceptions being [2,3,4]. In the final remarks, the review suggested that the journey towards the development of a set of comprehensive reliable models for self-healing cementitious materials was in its early stages.

In the five years since this review was published, substantial progress has been made on the above issues. There have been some significant combined experimental-numerical studies aimed at developing models for SCHMs. Cibelli et al. [5] developed a new discrete hygro-thermo-chemical model for simulating the behaviour of enhanced autogenous healing systems. This was a further development of the formulation developed by Di Luzio et al. [3], which employed the lattice discrete particle model. In this model, healing is simulated via a curing function that accounts for crack opening and temperature effects, the latter using an Arrhenius type term. The model was developed, calibrated and validated using data from the authors' group in Milan. The model predictions of the mechanical regain were found to be in good agreement with experimental results.

Romero Rodríguez et al. [6] explored the crack-sealing behaviour of cementitious materials containing

superabsorbent polymers (SAPs) in a combined experimental-numerical programme of work. The authors used a meso-scale lattice model to simulate coupled transport and mechanical behaviour. Richard's equation was employed to describe unsaturated moisture flow, with cracked elements having a higher diffusivity. An exponential equation was used to describe the hydraulic diffusivity as a function of moisture content in the cementitious matrix and a water absorption kinetics law was employed to simulate the sink term associated with the SAP particles. Cracking was modelled by element deactivation, using a standard lattice procedure for simulating fracture. The simulations predicted spatial moisture content distributions in the mortar matrix, and within the crack, along with the degrees of water absorption and SAP particle swelling. The results showed very agreement between the experimental measurements and the numerical results.

The authors' group made a detailed study of the processes governing the mechanical and transport behaviour of a vascular self-healing system in cementitious structural elements with cyanoacrylate (CA) as the healing agent. The experimental testing programme included mechanical tests on notched prismatic beams and notched cubes under direct tension [7]. The influence of the crack opening displacement (COD) and the curing time on the degree of healing were explored using tests with cracks that had fixed CODs during the healing period. The effect of the COD rate was examined using tests that had fixed COD rates and a continuous supply of healing agent. Another set of tests explored transport and curing properties [8]. The change in viscosity and meniscus angle were studied using a bespoke manometer. Curing was examined in a body of CA over a cementitious substrate. Sorption of

\* Corresponding author: [JeffersonAD@cardiff.ac.uk](mailto:JeffersonAD@cardiff.ac.uk)

CA through a natural crack surface in a concrete prism was also studied.

These experimental studies were used to guide the development of a new coupled finite element model for simulating structures formed from self-healing cementitious materials [9] [10] [11] [12]. The essential components of the model are described in Section 2 of this paper.

The approach was initially developed for simulating autonomic healing systems with CA as the healing agent but recently the range of problems to which the model is applicable has been broadened [12]. The problems considered in the most recent work include a vascular self-healing cementitious specimen with sodium silicate solution as the healing agent and autogenous healing within a cementitious specimen with and without crystalline admixtures. A first exploration of the ability of the model to simulate Microbially Induced Calcium Carbonate Precipitation (MICP) was also presented. The work reported in the present paper extends the previous work on modelling MICP to include a consideration of post-healed mechanical response.

In the remainder of this paper, Section 2 provides an overview of the main governing equations and assumptions used in the coupled model; Section 3 describes the curing front model and discusses its use for simulating of healing from MICP; Section 4 presents an example that considers healing derived from MICP in a set of ceramic specimens; and Section 5 draws some overall conclusions from the work.

## 2 Model governing equations

The model described in references [9] to [12] comprises coupled mechanical and transport components. The essential constituent of the mechanical component is a damage-healing constitutive model that governs the traction ( $\tilde{\sigma}$ ) versus relative-displacement ( $\tilde{\mathbf{u}}$ ) behaviour of an embedded interface within a specialised 3D finite element, which is illustrated in Figure 1. The constitutive equations for the uncracked bulk material and the damage-healing interface are given in equations (1) and (2) respectively:

$$\boldsymbol{\sigma} = \mathbf{D}_e(\boldsymbol{\varepsilon} - \boldsymbol{\varepsilon}_c) \quad (1)$$

$$\tilde{\boldsymbol{\sigma}} = (1 - \omega)\tilde{\mathbf{k}}^e \tilde{\mathbf{u}} + h \tilde{\mathbf{k}}^h (\tilde{\mathbf{u}} - \tilde{\mathbf{u}}_h) \quad (2)$$

where  $\boldsymbol{\varepsilon}$  is the continuum strain tensor,  $\boldsymbol{\varepsilon}_c$  is the strain in the continuum part of the element caused by the displacement jump at the discontinuity,  $\omega \in [0,1]$  is the crack-plane damage variable,  $h$  denotes the proportion of material that is healed at any one time,  $\tilde{\mathbf{k}}^e$  is the elastic stiffness of the material in the crack band,  $\tilde{\mathbf{k}}^h$  is the counterpart to  $\tilde{\mathbf{k}}^e$  for healed material and  $\tilde{\mathbf{u}}_h$  is the healing relative-displacement associated with cured material in open cracks.

The approach used to simulate re-damage and re-healing is explained in full in Reference [11]. This is based on equation (3):

$$h = (1 - \omega_h)h_v \quad (3)$$

in which the current degree of  $h$  is computed from the virgin damage variable ( $h_v$ ) and the proportion of  $h_v$  which has re-damaged ( $\omega_h$ )

Re-healing results in a reduction  $\omega_h$ . At each increment in the solution, the algorithm employs a damage sub-step, in which  $\omega$  and  $\omega_h$  are updated whilst  $h_v$  is fixed, and then a healing step in which  $h_v$  is updated and  $\omega_h$  reduced to account for any re-healing.

The method used to compute  $h$  for different healing systems is discussed in Section 3.

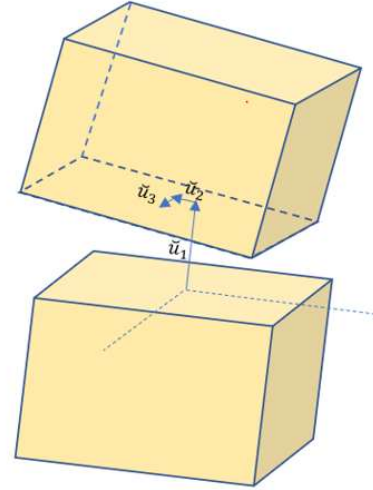


Fig. 1. 3D finite element with embedded discontinuity

Fluid transport processes are illustrated in Figure 2, and the associated main governing equations for flow within a discrete crack and within the surrounding matrix are given by equations (4a-d) and (5a-b) respectively:

$$\mathbf{v} = - \left( \frac{k_{crk} + 0.5\mu w_c \beta_w \beta_{vr}}{\mu} \right) (\nabla P_{crk} - \rho \mathbf{g}) \quad (4a)$$

$$\frac{\partial(\rho w_c)}{\partial t} + \nabla \cdot (\rho w_c \mathbf{v}) = 0 \quad (4b)$$

$$P_{crk} = P_c (1 - \beta_s) - 2 \frac{\beta_m}{w_c} \mathbf{v} \cdot \mathbf{n} \quad (4c)$$

$$P_{crk} = P_{app} \quad (4d)$$

$$\frac{\partial(\bar{\rho}_f)}{\partial t} + \nabla \cdot \mathbf{J}_f + \rho q_{mtx} = 0 \quad (5a)$$

$$\bar{\mathbf{n}} \cdot \mathbf{J}_f = q_c \quad (5b)$$

where (4a & b) apply in the crack space ( $\Omega_{crk}$ ), (4c) on the fluid surface ( $\Gamma_m$ ), (4d) at the crack boundary where pressure ( $P_{app}$ ) is applied, (5a) in the matrix bulk ( $\Omega_{mtx}$ ) and (5b) on the matrix boundary:  $\beta_m$  and  $\beta_s$  are meniscus and stick slip material parameters,  $P_{crk}$  is the fluid pressure in the crack,  $\mathbf{v}$  is the fluid flow velocity,  $\rho$  is the fluid density,  $\bar{\mathbf{n}}$  is a unit vector on the boundary;  $\bar{\rho}_f = \rho n S_f$  is the phase averaged density,  $S_f$  is the degree of fluid saturation and  $\mathbf{J}_f$  is the fluid flux.

Darcy's law is used to relate the flux to the pressure gradient, and van Genuchten's equation [13] is used for the  $S_f$  v  $P_f$  relationship. All of the other transport-related constitutive equations are given in references [9] and [11].

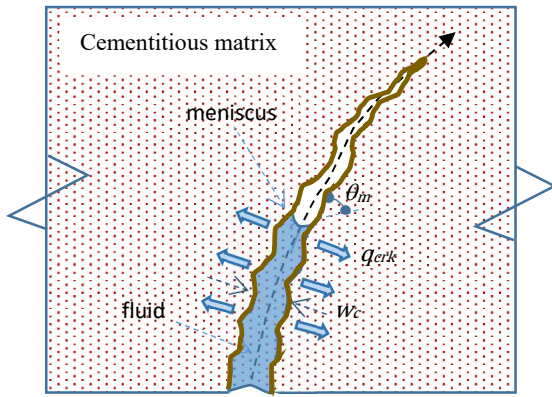


**Fig. 2.** Flow processes of a cementitious healing system

### 3 Curing, MICP and healing

The sub-model developed for healing in an autonomic vascular system with cyanoacrylate as the healing agent simulates advancing curing fronts from opposing crack faces within the body of healing agent. The degree of healing is computed from the overlap between these diffuse curing fronts [11], as illustrated in Figure 3. This figure represents the degree of cure ( $\phi$ ), at a distance  $x$  from a crack for a curing front at position  $\bar{z}$ , noting that  $\bar{z}$  is the generalised curing front variable derived from equation (5), such that in the absence of re-damage and re-healing,  $\bar{z} = z_f$ .

The model was derived by examining the chemical curing kinetics of cyanoacrylate and using observations and measurements from a number of experiments that studied the curing of CA on a cementitious substrate [7] & [8]. The healing function derived from this work, which depends on both the CMOD and its rate according to equations (6) to (8), is as follows:

$$z_f(t_c) = z_{c0} \left( 1 - e^{-t_c/\tau} \right) \quad (6)$$

$$h = \frac{\theta}{2} \left( 1 - \tanh \left( \frac{0.5w_c - \bar{z} - z_{c2}}{z_{c2} + \sqrt{\bar{z}/z_{c1}}} \right) \right) \quad (7)$$

$$\theta = \left( \frac{f_{stat} + f_{dyn}}{2} \right) - \left( \frac{f_{stat} - f_{dyn}}{2} \right) \cdot \tanh \left( \frac{w_c - w_{rt}}{w_{rnom}} \right) \quad (8)$$

where  $\bar{z}$  is the effective curing front variable derived from the curing front variable  $z_f$ ,  $z_{c0}$  is the critical curing depth,  $z_{c2}$  is a wall factor,  $z_{c1}$  is a diffusion constant, the static and dynamic factors are  $f_{stat} = 1$  and  $f_{dyn} = 0.45$  respectively,  $w_{rt} = 10^{-3} \zeta_m / \tau_h$  mm/s and  $w_{rnom} = w_{rt} / 10$ .

The idea of using the curing model to simulate healing in other types of healing system -and for a range of other healing agents- was discussed in Freeman et al. [12]. In the work described in the present paper, the approach is calibrated to simulate healing from MICP. In microbial healing, the healing material -usually calcium carbonate- grows from the crack walls. To predict this growth in detail, a kinetic bio-chemical sub-model would be required; however, we show here that a tractable alternative to such a model is to calibrate the parameters of the curing front function such that it represents microbial induced healing. The idea to use the model stems from observations of nano-scale simulations and MICP experiments [14], which show that -during a healing period- the average density of precipitate within a crack decreases with the distance from the crack face. This was considered analogous to the degree of cure within a body of liquid healing agent.

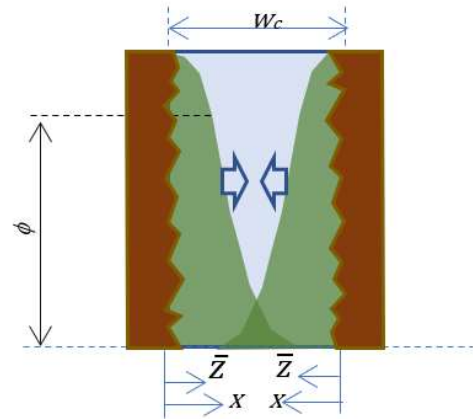


**Fig. 3.** Curing fronts emanating from crack walls

### 4 Example of MICP simulation

To validate the model, we consider the experimental data presented by Xin et al. [15]. In Xin et al.'s work, ceramic prisms of dimension  $24 \times 8 \times 2 \text{ mm}^3$  were pre-soaked with bacterial solution before being loaded in three-point bending to failure. Following this, the resulting two halves were fixed together with an interfacial gap of 0.3mm and immersed in a urea-CaCl<sub>2</sub> solution for different healing periods, before being reloaded to failure. The model parameters can be seen in Table 1, whilst the comparison between the numerical predictions and the experimental results of Xin et al. can be seen in Figures 4 and 5.

The curing front parameters ( $z_{c0}$ ,  $z_{c1}$ ,  $z_{c2}$  and  $\tau$ ) were calibrated to provide a close match with the experimental volume fractions of cured material [12] at different curing times. The mechanical and strength parameters ( $E$ ,  $\nu$ ,  $u_m$ ,  $f_t$  and  $f_{th}$ ) were either obtained directly from the experimental data [15] or, when not available, taken as typical values for the type of ceramic material used in the tests.

These values would need to be calibrated separately for MICP in another host material, or for a system which

used different bacteria; however, the overall approach should be applicable to MICP systems in general.

**Table 1.** Model parameters

Parameter	Value	Parameter	Value
$E$ (MPa)	175	$z_{c0}$ (mm)	0.9
$E_h$ (MPa)	290	$z_{c1}$ (mm)	20
$\nu, \nu_h$ (-)	0.3	$z_{c2}$ (mm)	0.00001
$f_t, f_{th}$ (MPa)	1.94	$\tau$ (days)	28
$u_m$ (mm)	0.0033	$w_c$ (mm)	0.3

It may be seen from the Figures that the model is able to accurately reproduce the experimental results both in terms of the healing strength ratio and the load-deflection response for different healing periods. Representative contours of the predicted vertical displacements immediately prior to fracture for the different healing periods can be seen in Figure 6.

It is noted that the ceramic material is relatively brittle, which is why no stable post-peak response is shown in the numerical results.

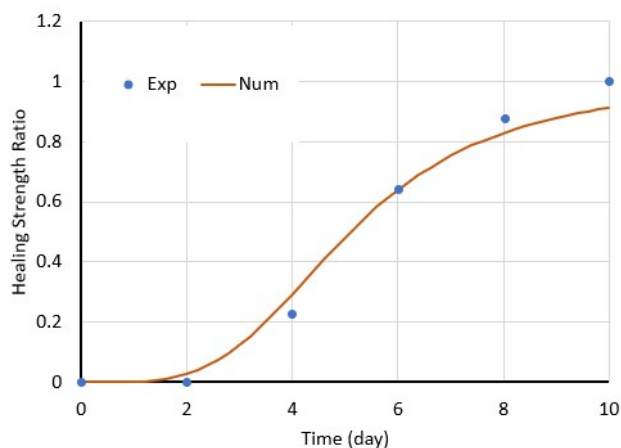


**Fig. 4.** Comparison of healing ratios

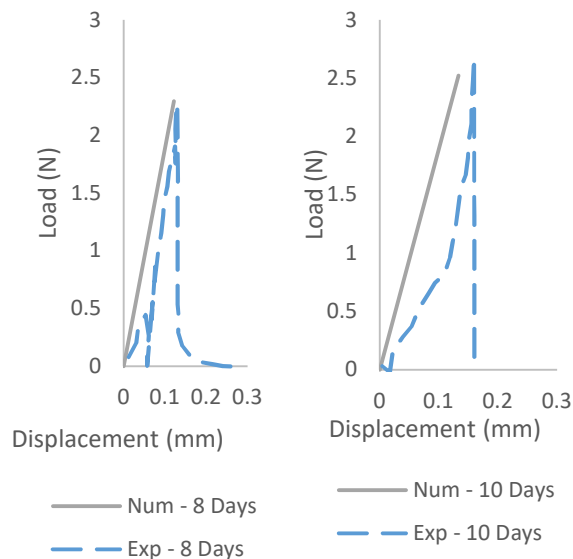
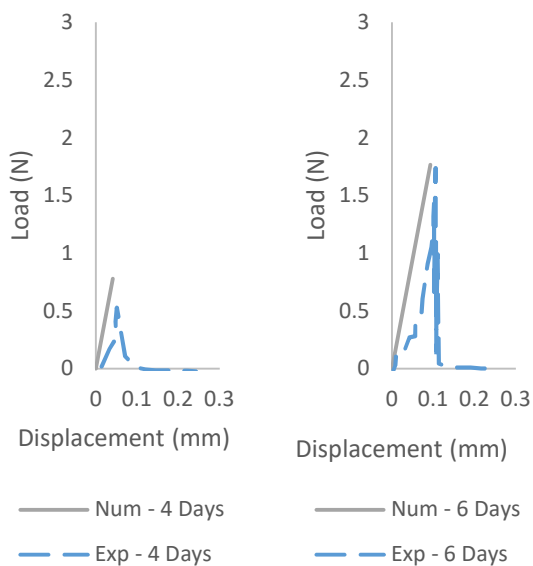


**Fig. 5.** Comparison between predicted load-deflection responses and the experimental results

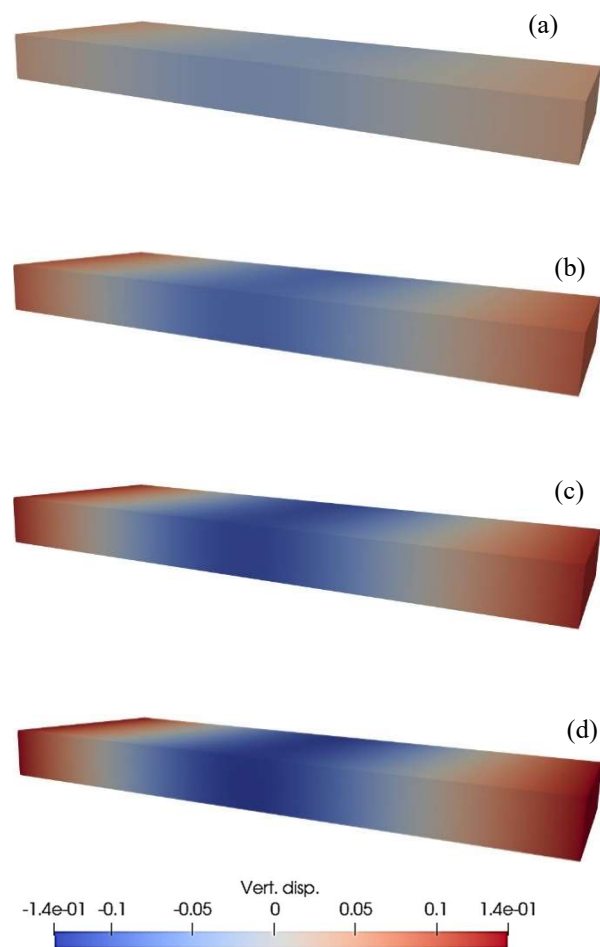


**Fig. 6.** Representative contours of vertical deflection prior to fracture after healing periods of a) 4, b) 6, c) 8 and d) 10 days

## 5 Conclusion

The results of these preliminary simulations of MICP in ceramic samples suggest that the curing front formulation, within the coupled finite element model developed by the authors, is an effective and pragmatic way of simulating cracking and healing in microbial-based healing systems.

Future work is well-progressed on a more fundamental model for predicting healing from MICP, which is informed from nano scale simulations [14].

Acknowledgements: Financial support from the UKRI-EPSCRC Programme Grant EP/P02081X/1 “Resilient materials for life (RM4L)” and EPSRC Standard Grant Engineering MICP via meso-Scale Simulations (Newcastle University EP/S013997/1; University of Bath EP/S013857/1; Cardiff University EP/S01389X/1) is gratefully acknowledged.

## References

1. A.D. Jefferson, E. Javierre, B. Freeman, A. Zaoui, E. Koenders, L. Ferrara. 2018. *Adv. Mater. Interfaces* **5**, 1–19. (2018)
2. B. Hilloulin, D. Hilloulin, F. Grondin F, A. Loukili, N. De Belie. *Cement and Concrete Research* **80**, 21–32 (2016)
3. G. Di Luzio, L. Ferrara and V. Krelani *Cement and Concrete Composites*, **86**, 190-205 (2018)
4. F.A. Gilabert, D. Garoz , W. Van Paepegem. *Materials & Design* **130**, 459–478 (2018)
5. A. Cibelli, M. Pathirage, G. Cusatis, L. Ferrara, G. Di Luzio., *Engineering Fracture Mechanics*, **263**, 108266. (2022)
6. C. Romero Rodríguez, S. Chaves Figueiredo, M. Deprez, D. Snoeck, E. Schlangen, B. Šavija, *Cement and Concrete Composites*, **104**, 103395 (2019)
7. T. Selvarajoo, R.E.Davies, B.L. Freeman, A.D. Jefferson. *Construction and Building Materials* **254**, 119245 (2020)
8. T. Selvarajoo, R.E. Davies, D.R. Gardner, B.L. Freeman, A.D. Jefferson. *Construction and Building Materials*, **245**, 118332, (2020)
9. B. Freeman, A.D. Jefferson. *Int. J for Num. and Anal. Meth. in Geo.* **44**(2), 293-326, (2020)
10. B.L. Freeman, P. Bonilla-Villalba, I.C. Mihai, W.F. Alnaas, A.D. Jefferson. 2020. *Adv. Model. and Simul. in Eng. Sci.* **7**, 32 (2020)
11. A.D. Jefferson and B.L. Freeman *Int. J. of Sol. and Strucs.*, **244–245**, 111601 (2022)
12. B.L. Freeman and A.D. Jefferson, *J Engn Mech. ASCE*, In Press, (2023). DOI 10.1061/JENMDT/EMENG-6944
13. van Genuchten MT. *Soil Science Society of America Journal.*; **44**(5):892 (1980)
14. M. Bagga, C. Hamley-Bennett, A. Alex, B. L. Freeman, I. Justo-Reinoso, I. C. Mihai, S. Gebhard, K. Paine, A. D. Jefferson, E. Masoero, I. D Ofițeru, *Construction and Building Materials*, **358**, 129412 ( 2022)
15. A. Xin, H. Du, K. Yu, Q. Wang. *Journal of the Mechanics and Physics of Solids*. **139** (2020) 103938